JACS
JOURNAL OF THE AMERICAN CHEMICAL SOCIETY
Article
pubs.acs.org/JACS

High-Throughput Synthesis and Electrochemical Screening of a Library of Modified Electrodes for NADH Oxidation

Aleksandra Pinczewska,[†] Maciej Sosna,[†] Sally Bloodworth,[†] Jeremy D. Kilburn,*[,‡] and Philip N. Bartlett*[,†]

[†]Chemistry, Faculty of Natural and Environmental Sciences, University of Southampton, Southampton SO17 1BJ, U.K.
[‡]School of Biological and Chemical Sciences, Queen Mary, University of London, Mile End Road, London E1 4NS, U.K.

Supporting Information

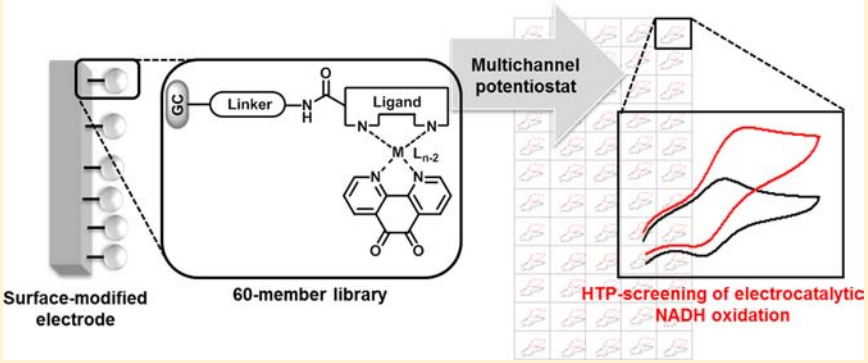

ABSTRACT: We report the combinatorial preparation and high-throughput screening of a library of modified electrodes designed to catalyze the oxidation of NADH. Sixty glassy carbon electrodes were covalently modified with ruthenium(II) or zinc(II) complexes bearing the redox active 1,10-phenanthroline-5,6-dione (phendione) ligand by electrochemical functionalization using one of four different linkers, followed by attachment of one of five different phendione metal complexes using combinatorial solid-phase synthesis methodology. This gave a library with three replicates of each of 20 different electrode modifications. This library was electrochemically screened in high-throughput (HTP) mode using cyclic voltammetry. The members of the library were evaluated with regard to the surface coverage, midpeak potential, and voltammetric peak separation for the phendione ligand, and their catalytic activity toward NADH oxidation. The surface coverage was found to depend on the length and flexibility of the linker and the geometry of the metal complex. The choices of linker and metal complex were also found to have significant impact on the kinetics of the reaction between the 1,10-phenanthroline-5,6-dione ligand and NADH. The rate constants for the reaction were obtained by analyzing the catalytic currents as a function of NADH concentration and scan rate, and the influence of the surface molecular architecture on the kinetics was evaluated.

INTRODUCTION

The deliberate modification of electrode surfaces by adsorbed or covalently attached molecules was first investigated almost 40 years ago in pioneering work by the groups of Hubbard[1] and Murray.[2,3] In the intervening period many groups have contributed to the development of a wide variety of approaches for the modification of electrode surfaces, to modeling of their properties, and development of their applications.[4−6]

The motivation for the modification of electrode surfaces is to achieve control over the properties of the electrode surface and to be able to tailor these to a specific application. Through monolayer modification of the electrode surface it is possible to control properties such as wetting,[7] cell adhesion,[8,9] protein adsorption,[10,11] accumulation of analytes for electroanalysis through stripping voltammetry,[12,13] and electrocatalysis of redox processes.[14,15]

Although many different modified electrodes have been studied, many of the subtleties of the effects of the immobilization method and surface molecular structure remain to be explored. An attractive way to do this is to learn from the field of high-throughput (HTP), or combinatorial, chemistry where the synthesis of small-molecule libraries using solid-phase synthesis on polymer supports has been widely used. In this approach the substrate is covalently attached to a polymer support through a linker, and after several synthetic steps the product is generally cleaved from the solid support and screened for the property or properties of interest.[16,17] For application to the synthesis of modified electrodes, the electrode surface simply replaces the polymer support, but importantly no cleavage of molecules from the surface is carried out before screening. Although high-throughput methods have been widely used in materials chemistry,[18,19] their applications in electrochemistry have been much more restricted and have mostly concentrated on the screening of materials for electrochemical applications.[20] Guschin et al. used a combina-

Received: July 27, 2012
Published: October 9, 2012

 © 2012 American Chemical Society

torial approach to prepare a range of Os electrodeposited redox polymers[21] and have screened these for application in enzyme electrodes,[22] but this represents the present extent of the applications in bioelectrochemistry.

Over the last 4 years we have been developing high-throughput approaches to the study of modified electrodes based on electrochemical amine oxidation or diazonium salt reduction to attach molecules with *tert*-butyloxycarbonyl-(Boc-)protected amine groups to carbon electrode surfaces.[23−25]

Modification of carbon electrode surfaces by amine oxidation[26] occurs through electrochemical generation of primary or secondary amine radical cations, which then form covalent bonds to the carbon surface, and a wide range of modified electrodes have been prepared by this method.[15,26−31] Electrochemical oxidation of diamines[33] can potentially provide carbon electrodes with an amine functionalized surface;[15,26,30] however, a significant drawback of the approach is that diamines can form polymeric chains or bridges on the carbon surface.[26,28] In our work we overcome this problem by using mono-Boc-protected diamines in the initial electrochemical oxidation step and then removing the Boc protecting group to generate a free amine for further surface chemistry.[32]

In the second approach, originally developed by Pinson et al.[33,34] and subsequently widely applied,[31] the electrochemical reduction of a diazonium salt is used to generate a reactive aryl radical which couples to the electrode surface, with the benefit that it is not restricted to carbon electrode surfaces. A variety of functionalized aromatic diazonium salts have been employed,[26,31] and further chemical modification of the electrode surface can be carried out when specific substituents (e.g., $-COOH$,[35] $-SO_3H$,[35] $-NMe_2$,[35] or $-CH_2Cl$[36,37]) are present on the aromatic ring and hence able to bond metal complexes[35] or enzymes[38] or act as potential supports for combinatorial chemistry.[36] A disadvantage of the approach, however, is the low stability and availability of diazonium salts bearing suitable functional groups. In addition, under some circumstances multilayers of substituted aromatic compounds can be formed by electrolysis of diazonium salts.[39,40] We have used 4-(*N*-Boc-aminomethyl)benzene diazonium tetrafluoroborate salt as a linker, and since the Boc group is readily removed by treatment with acid, this allows the introduction of an amine functionality to the surface which is not otherwise possible because of the reactivity of unprotected amines with diazonium salts. An alternative approach of attaching a nitro-substituted aryldiazonium, followed by reduction of the nitro group, is complicated by the difficulty of achieving full reduction of $-NO_2$ to $-NH_2$ at the electrode surface.[41] Our use of a bulky Boc protecting group discourages the formation of polymeric layers[23] on the surface by steric blocking of further coupling reactions at the 3- and 5-positions of the aromatic ring, preventing the buildup of multilayers.

In the present paper we concentrate on modified electrodes for oxidation of NADH. The NAD^+/NADH couple plays a key role in biological electron transfer as a two-electron, one-proton redox reagent and is relevant for the development of a wide range of substrate specific biosensors.

The oxidation of NADH is formally a H^- transfer,[42] but it has long been debated as to whether this occurs in a single step or in sequential steps.[43,44] The $E^{o\prime}$ for NAD^+/NADH is −0.315 V vs NHE at pH 7,[45−47] but at bare metal electrodes the oxidation of NADH shows significant irreversibility and requires overvoltages of up to 1 V;[48] thus, an ECE route for direct electrochemical oxidation of NADH has been proposed.[49] The use of high overpotential at unmodified electrodes for NADH oxidation leads to rapid fouling of the electrode and, if used in biosensor applications, causes problems from interference due to oxidation of other species present in the sample. The electrochemical oxidation of NADH is thus an ideal target for the development of modified electrodes (designed to catalyze the electrooxidation), and many examples have been described in the literature.[49−53]

The requirements for a mediator for NADH oxidation are stringent. It must significantly reduce the overvoltage for the reaction, ideally to around 0−0.2 V vs SCE for application in biosensors in order to avoid significant interference from oxidation of species such as ascorbate, urate, and acetomidophen present in typical biological samples such as whole blood and serum. At the same time it must maintain fast reaction kinetics (ideally with a second-order rate constant of the order of 10^6−10^7 $dm^3\ mol^{-1}\ s^{-1}$ or greater). The best mediators are molecules which can undergo reaction with NADH by hydride transfer followed by electrochemical reoxidation in two one-electron transfer steps, whereas species which can only undergo a one-electron reaction with NADH are poor mediators.[50,54]

Herein, we use 1,10-phenanthroline-5,6-dione (phendione)[55] complexes as mediators for NADH oxidation. Phendione forms a stable complex with a wide variety of transition metals[56] to give a positively charged mediator. Such complexes have been adsorbed on graphite[56d,i] and glassy carbon,[56a] attached to gold,[56h] mixed with carbon paste,[56b,k] or electropolymerized at the electrode surface[56a] to give modified electrodes for NADH oxidation which show good reactivity and stability. In this work we report studies using phendione complexes that are covalently attached to the electrode surface, and prepare a library of three replicates of each of 20 different modified electrodes using five different complexes and four different attachments. Using a high-throughput approach we investigate the electrochemistry of this library and the application of the different modified electrodes for the oxidation of NADH by studying the reaction at different NADH concentrations and scan rates. Using an established kinetic model for the oxidation of NADH at modified electrodes, the data are analyzed to extract K_M and k_{cat} values for the different modified electrodes. This significantly extends our earlier preliminary study of a library of dihydroxybenzene derivatives[57] and enables us to explore the effects that the different complexes and attachments have on the reaction kinetics.

■ RESULTS AND DISCUSSION

Design and Synthesis of the Library of Modified Electrodes. Covalent functionalization of glassy carbon (GC) electrodes was based on methodology developed by Kilburn and Bartlett for control of the molecular architecture on a carbon surface, using sequential electrochemical and solid-phase synthesis methods.[23,24,32,57] Our general approach involved initial coupling of a linker bearing *N*-Boc-protected amine functionality to the GC electrode, using either electrochemical oxidation of a primary amine[26,28,29] or reduction of a diazonium salt,[26,33,34] followed by *N*-deprotection to give a free amine at the electrode surface suitable for amide-coupling with a metal chelating ligand bearing carboxylic acid functionality.[23,24,32,57] Following coupling to the ligand, chelation of a reactive metal complex was carried out. Hence, we were able to design and prepare a library of modified electrodes which would allow us to assess the

Scheme 1. Sequential Electrochemical and Solid-Phase Synthesis Strategy for Covalent Immobilization of Metal Complexes at the GC Electrode Surface

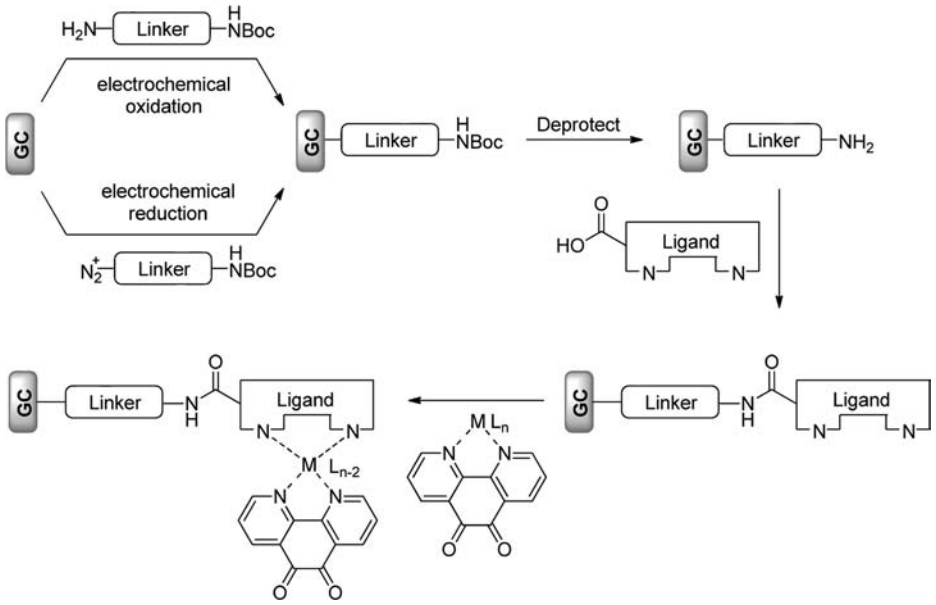

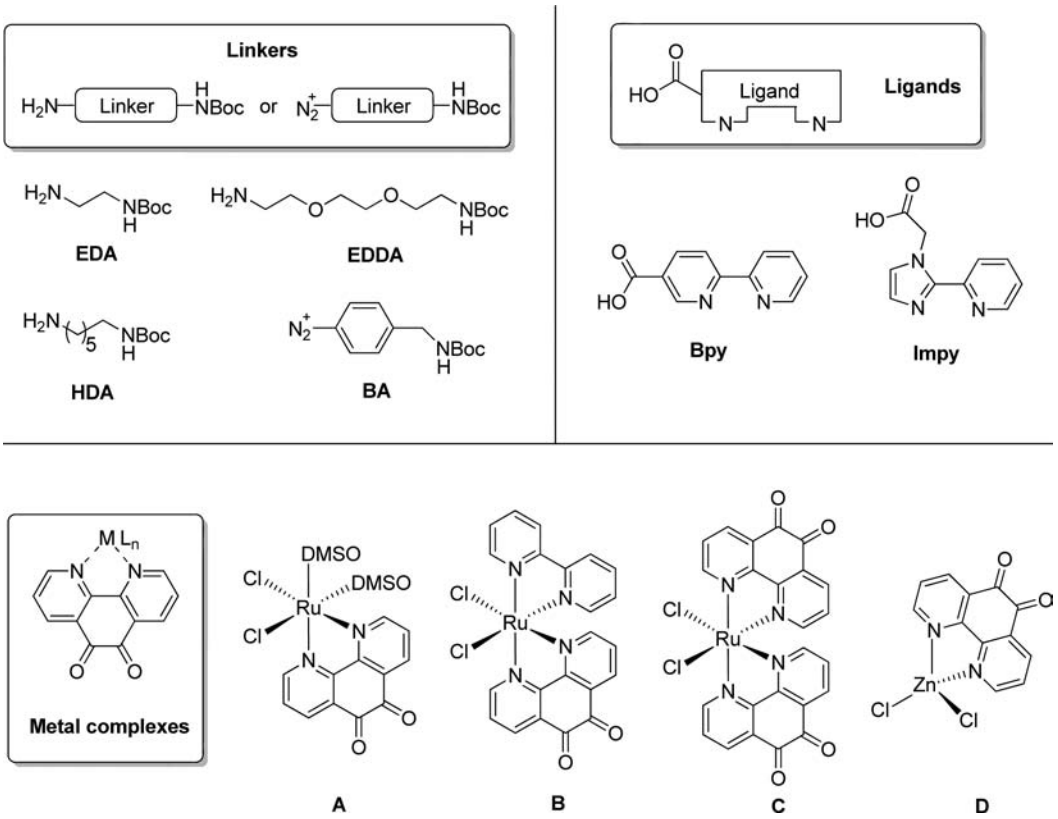

Figure 1. Structures of linkers, chelating ligands, and metal complexes used for preparation of the library of 60 modified electrodes; *linkers*: **EDA** (1,2-ethylenediamine), **HDA** (1,6-hexanediamine), **EDDA** (2,2′-(ethylenedioxy)diethylamine), and **BA** (*p*-benzylamine); *chelating ligands*: **Bpy** (2,2′-bipyridine-5-carboxylate), **Impy** (2-(1-(carboxymethyl)-1*H*-imidazol-3-ium-2-yl)pyridin-1-ium), *metal complexes*: complex **A** ((dimethyl sulfoxide)(1,10-phenanthroline-5,6-dione) ruthenium(II) chloride), complex **B** ((2,2′-bipyridine)(1,10-phenanthroline-5,6-dione) ruthenium(II) chloride), complex **C** (bis-(1,10-phenanthroline-5,6-dione)ruthenium(II) chloride), complex **D** (1,10-phenanthroline-5,6-dione zinc(II) chloride).

effects on NADH catalytic oxidation of varying the linker unit, the geometry of the metal complex, and the steric and electronic effects of the ligands attached to the metal center (Scheme 1).

Four linkers were selected to investigate the effect of variation in their length, flexibility and chemical functionality upon both the surface coverage of the attached metal complex and the catalytic activity of the resulting modified electrodes. In order to study the effect of different metal centers and

Table 1. Design of the Library of 20 Different Modified Electrodes 1−20 with Each Modification Prepared in Triplicate (copies a−c)[a]

Metal Complex	Linker: EDA	Linker: HDA	Linker: EDDA	Linker: BA	Ligand
A	1 a-c	2 a-c	3 a-c	4 a-c	Bpy
B	5 a-c	6 a-c	7 a-c	8 a-c	Bpy
C	9 a-c	10 a-c	11 a-c	12 a-c	Bpy
D	13 a-c	14 a-c	15 a-c	16 a-c	Bpy
D	17 a-c	18 a-c	19 a-c	20 a-c	Impy

[a]COLUMNS represent variation in the linker: **EDA**, **HDA**, **EDDA**, or **BA**; ROWS represent variation in the metal complex (ruthenium complexes **A**−**C** or zinc complex **D**) and also the chelating ligand **Bpy** or **Impy**.

geometry of the metal complex on the electrochemical and electrocatalytic properties of functionalized GC electrodes, two different chelating ligands 2,2′-bipyridine (**Bpy**) and 2-(imidazolyl)pyridine (**Impy**), three different octahedral ruthenium complexes **A**−**C**, and the tetrahedral zinc complex **D**[58−60] were chosen. The three octahedral ruthenium complexes **A**−**C** would enable us to vary the combination of chelating ligands attached to the ruthenium metal ion and hence the steric bulk of the complex, accessibility of the active phendione moiety, and the electronic properties of the ruthenium metal center (Figure 1).

Preparation of 20 different modified electrodes **1**−**20** was planned, utilizing various combinations of linker, ligand and metal complex, with each electrode prepared in triplicate (**a**-**c**) in order to test reproducibility of the electrode performance (Table 1). It was anticipated that HTP Electrochemical

Screening of the Library of 60 modified GC electrodes would allow direct and rapid comparison of the different modifications, during a single set of measurements, and hence rapid identification of the best modification in respect of the surface coverage and catalytic activity toward NADH oxidation.

In order to determine suitable reaction conditions for multistep, sequential functionalization of GC electrodes, a single modified electrode, **1**, was initially prepared (Scheme 2).

Scheme 2. Sequential Electrochemical and Solid-Phase Preparation of Electrodes 1−20[a]

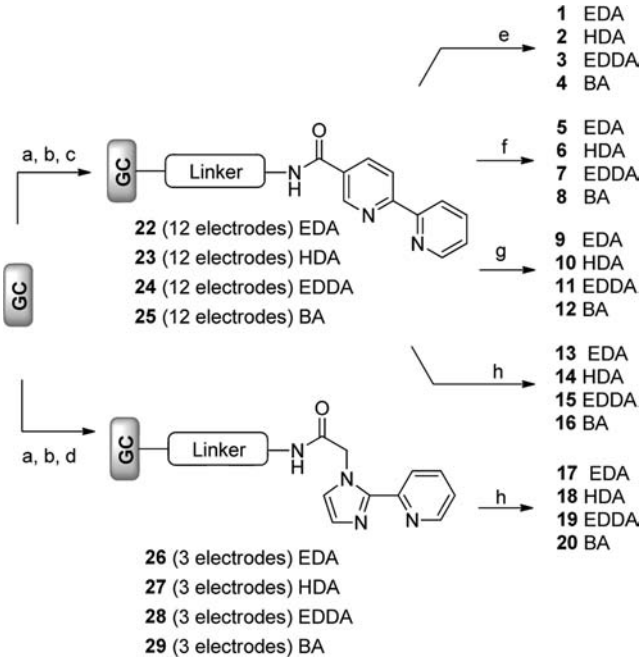

[a]Reagents and conditions: Prior to modification, 3 mm diameter (0.071 cm^2) glassy carbon (GC) rod electrodes were individually polished with silicon carbide paper (grade P1200, 3M). a) 15 mM solution of mono-*N*-Boc diamine linker in acetonitrile with 0.1 M TBATFB, from 0 to 2.25 V vs Ag/AgCl at a scan rate of 50 mV s^{-1} for attachment of linkers **EDA**, **HDA**, and **EDDA**; or 15 mM solution of (*N*-Boc-aminomethyl)benzene diazonium tetrafluoroborate salt in acetonitrile with 0.1 M TBATFB, 0.6 to −1 V vs Ag/AgCl at a scan rate of 50 mV s^{-1} for the **BA** linker; b) 4.0 M HCl in 1,4-dioxane, 1 h, room temperature; c) 1.0 M solution of 2,2′-bipyridine-5-carboxylic acid (1 equiv.) in DMF, HBTU (1.2 equiv), DIEA (4.2 equiv.), room temperature, 16 h, d) 1.0 M solution of 2-(1-(carboxymethyl)-1*H*-imidazol-3-ium-2-yl)pyridin-1-ium trifluoroacetate salt (1 equiv.) in DMF, HBTU (1.2 equiv), DIEA (10 equiv), room temperature, 16 h, e) complex **A**, DMF, 100 °C, 16 h; f) complex **B**, DMF, 100 °C, 16 h; g) complex **C**, DMF, 100 °C, 16 h; h) complex **D**, DMF, 50 °C, 16 h.

Hence, mono-*N*-Boc-ethylenediamine (mono-*N*-Boc-EDA) was oxidized at the GC electrode surface leading to a full monolayer, **21**, with an estimated surface coverage[32] of ∼1200 pmol cm^{-2}. *N*-Deprotection of electrode **21** was then carried out and although the resulting modified electrode bearing free amine functionality was not directly characterized, essentially quantitative deprotection can be inferred from our previous work and the well-established reliability of this reaction in solution.[23,24,32,S7] Reaction of the free amino electrode with 2,2′-bipyridine-5-carboxylic acid under solid-phase peptide coupling conditions gave electrode **22**, bearing a 2,2′-bipyridine chelating ligand. Finally, electrode **22** was treated with a solution of bis-(dimethyl sulfoxide)(1,10-phenanthroline-5,6-dione) ruthenium(II) chloride[58] (complex **A**) to obtain functionalized electrode **1**. Conditions for chelation of the metal complex to the surface-immobilized ligand were optimized by performing the solid-phase attachment of **A** to **22** at various reaction temperatures (between 25 and 154 °C) and reaction times (from 4 to 16 h). The newly formed ruthenium complex at electrode **1** was characterized by cyclic voltammetry in aqueous solution, for which a reversible redox peak at potential E_{mp} of −60 mV vs SCE was observed, corresponding to $2H^+/2e^-$ redox process of the phendione ligand (Figure 2). Surface coverage Γ for electrode **1** was

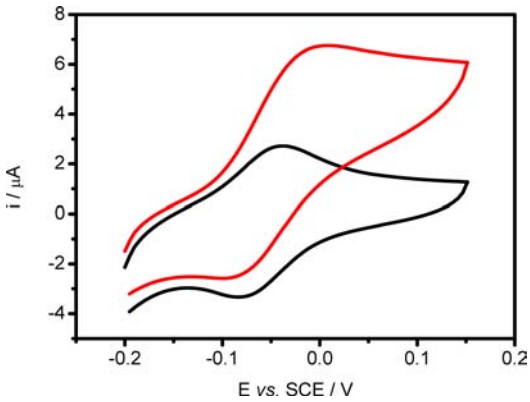

Figure 2. Cyclic voltammograms of electrode **1** recorded in 0.1 M phosphate buffer pH 7 in the absence (black curve) and in the presence (red curve) of 1 mM NADH at a scan rate of 50 mV s^{-1}.

estimated according to Faraday's law,[59] as Γ ∼110 pmol cm^{-2}, corresponding to the estimated theoretical surface coverage for a monolayer of related osmium complexes.[60] Since coverage of EDA-*N*-Boc for electrode **21** was estimated at ∼1200 pmol cm^{-2}, subsequent *N*-deprotection, ligand coupling and metal complexation has taken place in an overall yield of ∼10%, presumably since the surface can only accommodate a maximum coverage of 110 pmol cm^{-2} of the bulky metal complex. The cyclic voltammogram recorded for electrode **1** in an aqueous solution of NADH (Figure 2) gave a catalytic anodic peak around 0 V vs SCE corresponding to the electrocatalytic oxidation of NADH mediated by the phendione ligands. The presence of phendione (*o*-benzoquinone moiety) at the GC reduces the overpotential by ∼0.4 V relative to oxidation of NADH at the bare carbon electrode (0.4 V vs SCE).[61,62]

Having successfully developed the necessary synthetic and electrochemical approach for the preparation of a single modified electrode **1** and shown it to be an effective electrocatalyst for NADH oxidation, we applied the method to preparation of the library of 60 electrodes **1−20** (**a−c**). Preparation of bare electrodes and initial linker-attachment was carried out individually for each of the 60 electrodes. Solid-phase coupling of the ligand and metal complex were then performed using parallel and combinatorial methods to minimize the overall number of synthetic operations. Each of the 60 blank electrodes were electrochemically modified with EDA, HDA or EDDA linker by electrochemically assisted oxidation of primary amines according to the previously described procedure, or with BA linker by electrochemical reduction of the diazonium salt.[23,63] Simultaneous *N*-Boc deprotection of all 60 electrodes was carried out by applying the reaction conditions described for preparation of electrode

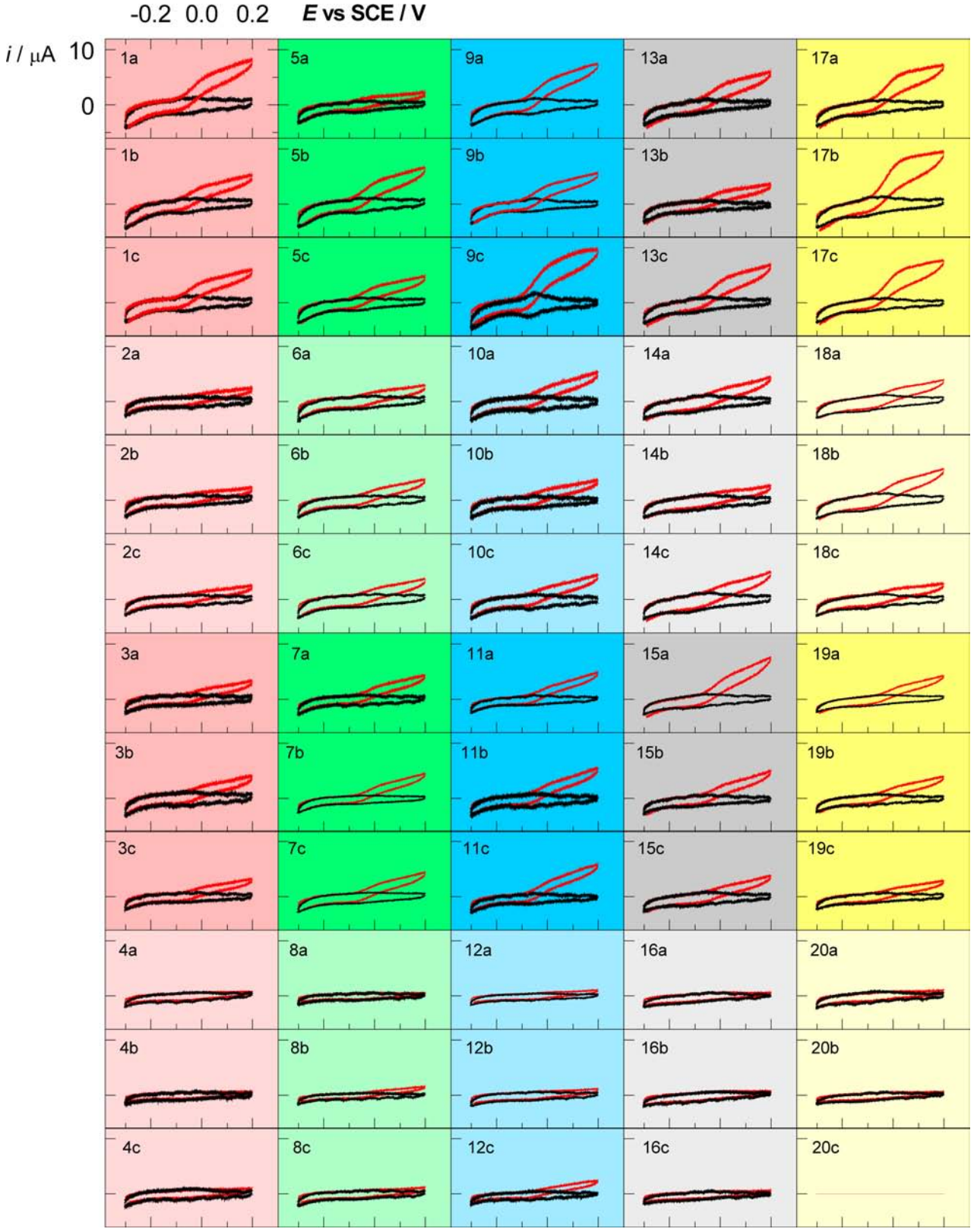

Figure 3. Cyclic voltammograms for the library of 60 modified electrodes in pH 7, 0.1 M phosphate buffer in the absence (black) and in the presence (red) of 4 mM NADH at a scan rate of 10 mV s^{-1}.

1.[23,32,57] The resulting free amines were coupled with 2,2′-bipyridine-5-carboxylic acid to give electrodes **22**−**25** (12 replicates) or with 2-(1-(carboxymethyl)-1*H*-imidazol-3-ium-2-yl)pyridin-1-ium trifluoroacetate salt[64] to give modified electrodes **26**−**29** (3 replicates) (Scheme 2). For these coupling reactions all electrodes were dipped in a bulk solution of appropriate ligand, coupling reagent and base for the same period of time and the solid-phase coupling reactions were

performed simultaneously in order to minimize differences resulting from possible decomposition of functionalized GC electrodes over time. Finally, electrodes **22**−**29** were treated with complex **A**, **B**, **C**, or **D** under reaction conditions which were optimized using individual GC electrodes and based on literature methodologies for formation of the ruthenium and zinc complexes in solution.[65−67] These solid-phase attachments of different metal complexes were performed in parallel. Four-neck reaction vessels enabled four electrodes to be placed in a sealed flask to allow immobilization of a given complex on four electrode surfaces simultaneously. We restricted these reactions to four electrodes in order to ensure a uniform temperature within the reaction vessel and the reproducibility of the modifications. One each of electrodes **22**−**25** was placed in a reaction vessel containing a solution of the appropriate metal complex, and similarly for one each of electrodes **26**−**29**. The arrangement was repeated for each of the 12 copies of electrodes **22**−**25** and three copies of **26**−**29**, giving three copies (**a**−**c**) of each of the 20 different electrodes **1**−**20**. Importantly the three copies of each modification were prepared in separate reaction vessels to ensure that if any significant synthetic problems occurred in one of the reaction flasks, it would only affect a single copy of any one electrode structure and hence should show up clearly in subsequent measurements of the properties of the full library of electrodes. All the reactions were performed at the same time so that any decomposition of the modifications with time was consistent for all electrodes.

HTP Electrochemical Screening of the Library. The resulting library of 60 electrodes was electrochemically characterized in high-throughput mode using a multichannel potentiostat. Electrocatalytic activities toward NADH oxidation were investigated in order to evaluate the effects of different linkers and complexes on the catalytic process. An example of a series of voltammograms recorded in the absence and presence of NADH is shown in Figure 3. A full set of data is given in the Supporting Information (Figures S1−S20). Figure 3 allows immediate visual identification of the "best" of the 20 different modified electrodes for NADH oxidation; in this case modified electrode **17**. However a more detailed analysis is required to extract the coverage and reaction kinetics which are of interest if we wish to pursue a rational design of better electrodes for NADH oxidation.

From the voltammetry in the absence of NADH the peak separation, midpeak potentials and the surface coverages can all be evaluated. Over the scan rate range 10−500 mV s^{-1} the peak currents were found to vary linearly with scan rate, as expected for a surface-bound redox couple. The midpeak potentials E_{mp} and peak separations ΔE_p are given in Table 2.

The midpeak potentials for the three octahedral Ru complexes attached through the four different linkers are very similar (−55 ± 5 mV vs SCE at pH 7), showing that the phendione electrochemistry is unaffected by the nature of the other ligands around Ru, and are consistent with those reported for the phendione in $[Ru(phendione)_3]^{2+}$ in aqueous solution.[56a] For the tetrahedral Zn complexes the redox potentials are slightly more negative but are again all very similar (−83 ± 8 mV vs. SCE). This slight (∼30 mV) cathodic shift reduces the thermodynamic driving force for the oxidation of NADH and might therefore be expected to reduce the rate of reaction. We return to this point below when we discuss the NADH reaction kinetics. The voltammetric peak separations are an indication of the overall rate of the coupled electron and proton transfer between the electrode and the phendione. For the Ru complexes linked through the diamine linkers (**EDA**, **HDA**, and **EDDA**) the peak separations at 50 mV s^{-1} are all around 56 mV with a slightly higher value, ∼80 mV, for the diazonium linker; for the Zn complexes the peak separations are a little larger, ∼115 mV, with no significant difference between the diamine and diazonium linkers.

Table 2. Summary of Peak Separations (ΔE_p) and Mid Peak Potentials (E_{mp}) for Functionalized Electrodes 1−20.[a]

		Linker			
		EDA	HDA	EDDA	BA
1-4	ΔE_p / mV	45	58	51	83
	E_{mp} *vs.* SCE / mV	−56	−52	−50	−56
5-8	ΔE_p / mV	53	65	67	84
	E_{mp} *vs.* SCE / mV	−60	−50	−54	−52
9-12	ΔE_p / mV	45	49	50	72
	E_{mp} *vs.* SCE / mV	−61	−58	−59	−56
13-16	ΔE_p / mV	93	108	113	139
	E_{mp} *vs.* SCE / mV	−91	−89	−91	−75
17-20	ΔE_p / mV	88	121	132	112
	E_{mp} *vs.* SCE / mV	−91	−90	−77	−91

[a]Obtained from cyclic voltammograms recorded at 50 mV s^{-1} in 0.1 M, pH 7.0 phosphate buffer. The values are averaged for three replicate electrodes with approximate estimated errors ∼±3 mV.

Surface coverage (calculated from voltammetry, Figure 4) is clearly related to the size of the immobilized metal complex at the surface. Hence, electrodes modified with the smaller tetrahedral zinc(II) complexes tend to show higher coverage for a given linker than electrodes modified with the bulkier ruthenium(II) complexes. Among the Ru complexes, highest coverage for any given linker is found for **1**−**4**, which contain two relatively small chloride ligands. Substitution of the chloride by the more bulky **Bpy** or phendione bidentate ligands (modifications **5**−**12**) decreases the surface coverage.

The use of linkers with different structures and chain lengths also influences the surface coverages obtained for a given metal complex. In earlier work we have shown that the coverage of diamine linkers on GC electrodes decreases with the increase in length of the aliphatic chain.[32] The presence of the longer aliphatic chain in the diamine is assumed to cause conformational disorder which prevents the access of free amine groups to the carbon surface and hinders covalent bond formation as the electrochemical oxidation proceeds.[30] Lower surface

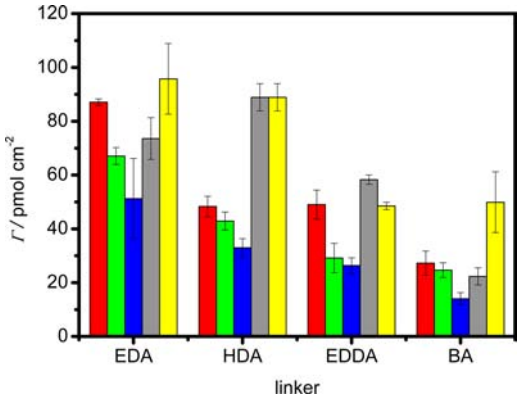

Figure 4. Mean values (n = 3) of the surface coverage of phendione ligand (Γ) for the library of 60 GC electrodes; modifications **1**−**4** (red bars), **5**−**8** (green bars), **9**−**12** (blue bars), **13**−**16** (gray bars), and **17**−**20** (yellow bars).

coverage of the linker may lead to a decrease in the amount of ligand subsequently attached to the linker and in the amount of metal complex formed in the final step. However, since only 10% of the available amine sites are required for coupling on the EDA surface (vide supra), a significant reduction in surface coverage of the linker could be tolerated without necessarily affecting coverage of the final metal complex. It therefore seems probable that conformational disorder and entanglement of the aliphatic chains, using the longer chain linkers, also affects the efficiency of subsequent coupling reactions, with the amine head groups of the deprotected linkers being buried or sterically inaccessible. This problem may become more pronounced after attachment of the ligand (**Bpy** or **Impy**), leading to lower coverages of the final metal complexes.

Relatively low surface coverages were also obtained for electrodes modified by the BA linker. Here the limited flexibility of the linker presumably limits the ability of the 2,2′-bipyridine ligand to coordinate to the metal ion of the large complex. Hence, overall, the length and flexibility of the linker and the geometric arrangement of the metal complex at the surface all affect the surface coverage for the different modifications, and coverage can vary quite markedly with relatively small changes to these variables.

The library was screened in solution with NADH at pH 7 to assess the ability of the modified electrodes to catalyze the oxidation of NADH. Sample results are shown by the red curves in Figure 3 and show that the overpotential for NADH oxidation is significantly decreased compared to a bare glassy carbon electrode.[68] In each case catalytic oxidation of NADH is observed at the potential of the immobilized mediator. This confirms that the surface-bound phendione ligands are able to mediate the NADH oxidation, consistent with published work on adsorbed phendione complexes.[56a,b,h,i,k] In order to assess the role the particular linker−metal complex combination plays, the kinetics of the catalytic process at each modified electrode were characterized.

Previous work with a variety of mediators[49] has shown that the electrocatalytic oxidation of NADH can be described by a mechanism in which the NADH forms a reaction complex with the mediator followed by oxidation of the NADH and reduction of the mediator in the reaction complex. This reaction scheme can be written

$$\mathrm{NADH}_\infty \xrightarrow{k'_D} \mathrm{NADH}_0 \tag{1}$$

$$[\mathrm{Q}] + \mathrm{NADH}_0 \overset{K_M}{\longleftrightarrow} [\mathrm{Q{\cdot}NADH}] \tag{2}$$

$$[\mathrm{Q{\cdot}NADH}] \xrightarrow{k_{cat}} [\mathrm{QH^-}] + \mathrm{NAD}_0^+ \tag{3}$$

$$[\mathrm{QH^-}] + \mathrm{H^+} \rightarrow [\mathrm{QH_2}] \tag{4}$$

$$[\mathrm{QH_2}] \xrightarrow{k'_E} [\mathrm{Q}] + 2\mathrm{e^-} + 2\mathrm{H^+} \tag{5}$$

$$\mathrm{NAD}_0^+ \xrightarrow{k'_D} \mathrm{NAD}_\infty^+ \tag{6}$$

where [Q] and [QH_2] represent the oxidized and reduced forms of the bound phendione and the subscripts ∞ and 0 denote the bulk and electrode surface, respectively. In these equations k'_D is the mass transport rate constant (cm s^{-1}), and K_M and k_{cat} respectively describe the formation of the reaction complex between the NADH and surface-bound phendione and the oxidation of the NADH in the reaction complex. In writing the reaction scheme we have ignored any potential effects of partition or diffusion of NADH in a modified layer at the electrode surface because we are dealing with monolayer-modified electrodes. The reoxidation of the phendione at the surface is described by the electrochemical rate constant k'_E. In the analysis which follows we assume that k'_E is sufficiently fast so as not to be rate determining at the overpotentials used. This assumption is supported by the measured peak separations for the immobilized phendione complexes reported above. A kinetic treatment of the mechanism described here has been discussed in the literature for heterogeneous redox catalysis.[69] From that analysis, the catalytic current can be expressed as

$$i = nFA\frac{k'_D}{2}\left\{(K_{ME} + c) - \sqrt{(K_{ME} + c)^2 - 4k'_{ME}K_{ME}c/k'_D}\right\} \tag{7}$$

where c is the bulk concentration of NADH and k'_{ME} and K_{ME} are respectively the effective electrochemical rate constant and apparent Michaelis constant for the redox mediator modified electrode and are related to k_{cat} and K_M by

$$k_{cat} = K_{ME}k'_{ME}/\Gamma \tag{8}$$

and

$$K_M = K_{ME}(1 - k'_{ME}/k'_D) \tag{9}$$

In order to use eq 7 to analyze the catalytic responses we need to know the value of the mass transport rate constant k'_D. For a rotating disk or microelectrode, where mass transport is under steady-state conditions, this is well-defined. For a stationary electrode in cyclic voltammetry the diffusion layer thickness, and hence k'_D, changes as the potential is scanned in the experiment. In order to define k'_D for the stationary modified electrode we return to the expression for the current as a function of potential given by Nicholson and Shane[70] (eq 25 in their paper)

$$i_p = nFAc\sqrt{\pi Da}\,\chi(at) \tag{10}$$

where a is the dimensionless scan rate

$$a = nF\nu/RT \tag{11}$$

D is the diffusion coefficient of NADH, ν is the scan rate, and all other symbols have their usual meaning.

Recognizing that

$$k'_D = \frac{i}{nFAc} \tag{12}$$

we obtain

$$k'_D = \sqrt{\pi Da}\chi(at) = \left(\frac{DnFv}{RT}\right)^{1/2}\sqrt{\pi}\chi(at) \tag{13}$$

Taking the values of $\sqrt{\pi\chi(at)}$ corresponding to the peak current for the forward scan we obtain[70]

$$k'_D = 0.4463\left(\frac{DnFv}{RT}\right)^{1/2} \tag{14}$$

This value was used in the analysis of the data. It is worth noting that the analysis is not strongly dependent on the precise value of k'_D used; a variation in k'_D of 10% resulted in an average variation in the corresponding values of k_{cat} and K_M of the order of 0.5% and 3%, respectively. This uncertainty can be considered negligible as compared to the experimental errors and does not alter the relative values for the different electrodes and therefore the conclusions presented below.

To gain insight into the kinetics of the catalytic reaction, cyclic voltammograms were recorded at 10, 20, 50, and 100 mV s^{-1}, corresponding to four distinct values of k'_D. The measurements were performed for varying concentrations of NADH, up to 4 mM. Shown in Figure 5 is an example of a family of voltammograms obtained, in this case, for the electrode **1** in solutions of increasing concentration of NADH.

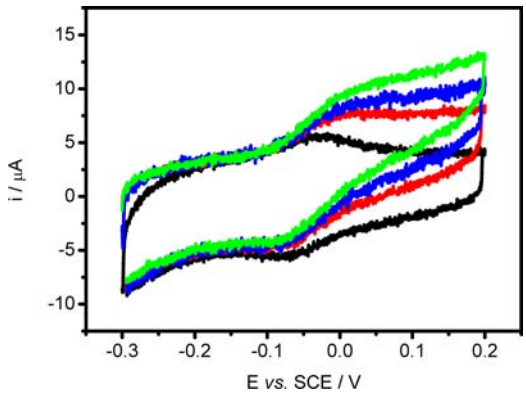

Figure 5. Example of cyclic voltammograms recorded with modified GC electrode **1** in 0.1 M phosphate buffer pH 7 at a scan rate of 50 mV s^{-1} and different NADH concentrations: (black line) 0, (red line) 1, (blue line) 2, and (green line) 4 mM.

The catalytic currents were then used to obtain plots of i_{cat} as a function of concentration of NADH for different values of scan rate and the data fitted to eq 7 to obtain the values for k'_{ME} and K_{ME} (see the example for **1** in Figure 6). Subsequently, values of k_{cat} and K_M were calculated using eqs 8 and 9 with the appropriate values for k'_D (calculated using a diffusion coefficient D value of 2.4×10^{-6} cm^2 s^{-1} for NADH in aqueous solution) and surface coverage of phendione ligands obtained by integration of voltammetric peaks in the absence of NADH. A full set of plots and the tabulated results for all 60 electrodes are given in the Supporting Information.

While the surface coverage of metal complex is the same as the coverage of phendione for modifications **1**−**8** and **13**−**20**, it is one-half the value for electrodes **9**−**12** which bear two phendione ligands. In the following analysis we assume that all the phendione ligands are equivalent and available to mediate

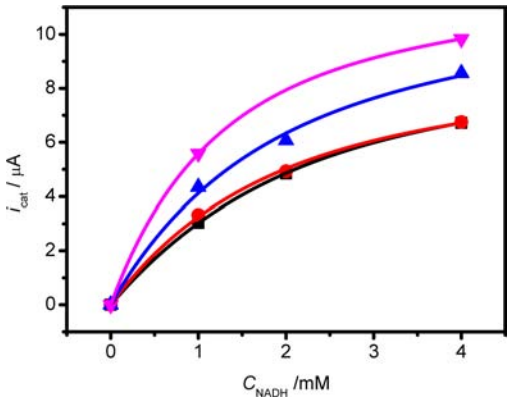

Figure 6. Catalytic currents for NADH oxidation as a function of NADH concentration for electrode **1** at a range of scan rates; (black-filled square) = 10, (red-filled circle) = 20, (blue-filled triangle) = 50 and (pink-filled heart) = 100 mV s^{-1}. The currents were determined from cyclic voltammograms in pH 7, 0.1 M phosphate buffer as a difference in current at 0.15 V vs SCE between NADH containing solution and NADH free solution. The lines are the least-squares fits of the experimental data to eq 7.

NADH oxidation, and therefore we use the ligand rather than metal complex coverages. The resulting kinetic parameters for all 20 different electrode modifications (obtained by averaging the three replicate measurements in each case) are summarized in Table 3 and compared graphically in Figures 7 and 8. For the complete set of voltammograms, plots of i vs c_{NADH} fitted with eq 7, as well as tables containing Γ, k'_{ME}, K_{ME}, k_{cat}, and K_M for each electrode the reader is referred to the Supporting Information (see Figures S1−S40 and Tables S1−S5).

To compare the kinetic results obtained here with those in the literature for phendione complexes reacting with NADH we need to introduce the apparent second-order rate constant, k_2, where

$$k_2 = k_{cat}/K_M \tag{15}$$

corresponds to the second-order rate constant for the reaction at low NADH concentration when the reaction sites are not saturated ([NADH] ≪ K_M).

The values for k_2 (Table 4) compare well with the published values for similar complexes of phendione. Thus, Wu et al.[56a] found values of k_2 of ∼4.4 mM^{-1} s^{-1} for [Ru(phendione)(4-vinyl-4′-methyl-2,2′-bipyridine)$_2$]$^{2+}$, ∼6 mM^{-1} s^{-1} for [Fe(phendione)$_3$]$^{2+}$, and ∼2.5 mM^{-1} s^{-1} for [Re(phendione)(CO)$_3$]$^+$ for electrodeposited films on glassy carbon measured at pH 7.2. Popescu et al.[56i] found values for k_{cat} and K_M of ∼0.8 s^{-1} and of ∼0.4 mM, respectively, giving a values of k_2 of ∼2 mM^{-1} s^{-1}, for drop-coated [Os(4,4′-dimethyl- 2,2′-bipyridine)$_2$(phendione)]$^{2+}$ adsorbed on spectrographic graphite and measured at pH 6.1, and Yokoyama et al.[56h] reported a value for a monolayer of [Ru(phendione)$_2$(5-amino-1,10-phenanthroline)]$^{2+}$ attached to Au of ∼1.2 mM^{-1} s^{-1} at pH 7.0. The values in Table 4 are also consistent with the linear free energy relationship for the reaction of NADH with various phenoxazine mediators (gallocyanine, ethyl capri blue, and methyl capri blue) reported by Gorton.[51]

On the basis of our high throughput study it is interesting to ask the question "which is the best modification for the oxidation of NADH?" On one level the answer to this question is simply obtained by looking at the raw data in Figure 3 where we can see that the largest catalytic currents are obtained for

Table 3. Kinetic Parameters for NADH Oxidation in pH 7.0, 0.1 M Phosphate Buffer for the Library of Modified Electrodes[a]

Electrode	Linker							
	EDA		HDA		EDDA		BA	
	k_{cat} / s^{-1}	K_M / mM	k_{cat} / s^{-1}	K_M / mM	k_{cat} / s^{-1}	K_M / mM	k_{cat} / s^{-1}	K_M / mM
1 – 4	7.3 ± 1.9	1.4 ± 0.2	3.7 ± 0.6	1.1 ± 0.2	6.6 ± 0.6	1.8 ± 0.1	2.4 ± 0.9	1.0 ± 0.4
5 – 8	7.8 ± 1.4	1.7 ± 0.2	6.6 ± 1.7	1.2 ± 0.2	15.3 ± 3.7	2.1 ± 0.2	1.6 ± 0.6	0.9 ± 0.1
9 –12	10.3 ± 0.4	2.3 ± 0.5	6.9 ± 1.3	1.9 ± 0.2	11.1 ± 0.4	2.2 ± 0.2	2.9 ± 0.3	1.1 ± 0.1
13 – 16	8.8 ± 1.2	2.0 ± 0.1	4.5 ± 1.3	1.7 ± 0.3	9.7 ± 3.8	2.3 ± 0.4	2.4 ± 0.3	0.4 ± 0.2
17 – 20	11.7 ± 1.3	2.6 ± 0.1	4.2 ± 0.8	1.8 ± 0.1	7.0 ± 1.4	1.5 ± 0.2	0.8 ± 0.1	0.3 ± 0.2

[a]The values are based on three replicates of each surface modification.

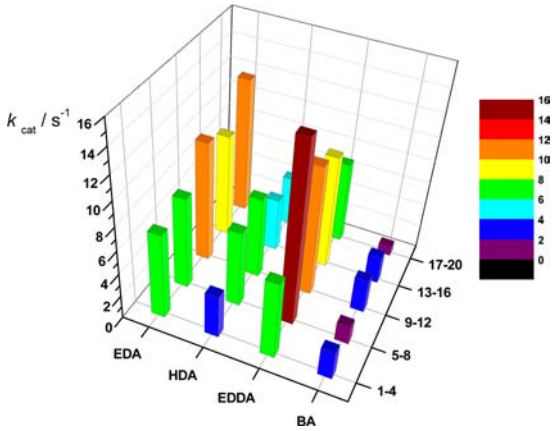

Figure 7. Comparison of k_{cat} for the reaction of phendione with NADH for the library of 60 electrodes **1–20 a–c**.

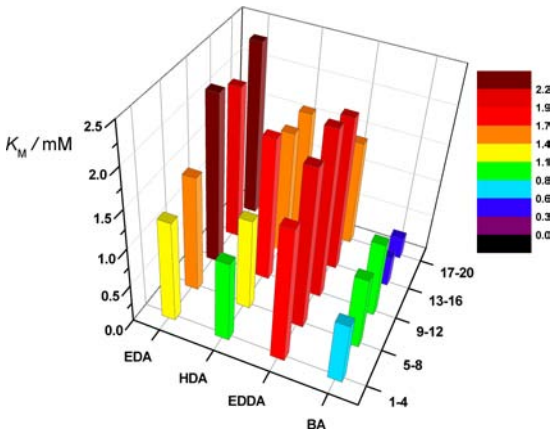

Figure 8. Comparison of K_M for the reaction of phendione with NADH for the library of 60 electrodes **1–20 a–c**.

modifications, **9** (using ruthenium complex **C** and the **Bpy** ligand) and **17** (using zinc complex **D** and the **Impy** ligand) both attached through the EDA linker. However, if we look at the values for k_2 in Table 4 the conclusion is different; the largest value for k_2 is found for modification **7** with ruthenium complex **B** and the EDDA linker. This difference arises because the k_2 values take account of the phendione coverage on the electrode surface and suggest that, provided the current increases linearly with the phendione coverage as assumed in our analysis, the optimum electrode could be achieved using the EDDA linker and complex **B** if the coverage on the electrode could be increased.

Table 4. Calculated Values for k_2 for NADH oxidation in pH 7.0, 0.1 M Phosphate Buffer for the Library of Modified Electrodes

Electrode	k_2 / mM^{-1} s^{-1}			
	EDA	HDA	EDDA	BA
1 – 4	5.2 ± 2.1	3.4 ± 1.2	3.7 ± 0.5	2.4 ± 1.9
5 – 8	4.5 ± 1.4	5.5 ± 2.3	7.3 ± 2.5	1.8 ± 0.9
9 – 12	4.5 ± 1.1	3.6 ± 1.1	5.0 ± 0.6	2.6 ± 0.5
13 – 16	4.4 ± 0.8	2.6 ± 1.2	4.2 ± 2.4	6.0 ± 3.8
17 – 20	4.5 ± 0.7	2.3 ± 0.6	4.7 ± 1.6	2.7 ± 2.1

The values of k_2, the apparent second-order rate constant for the oxidation of NADH, are made up of the contribution from K_M and k_{cat} (see eq 15). The equilibrium constant K_M (Figure 8) represents the strength of the intermediate complex formed between the NADH and the phendione moiety. The values of K_M calculated for all modifications containing aliphatic linkers show little variation and average around 1.8 mM. Within this group of modifications slightly lower values of K_M are observed only for electrodes with immobilized complex **A**. A significant decrease in K_M is observed for electrodes modified with the BA linker, which indicates that the phendione–NADH charge transfer complex is more stable for the mediators attached via BA compared to the aliphatic linkers. For the BA linker, the surface coverages of the metal complexes are low and therefore there is a high number of uncoordinated 2,2′- bipyridine ligands present at the surface. It is possible that the resulting local chemical environment around the mediator provides additional stabilization for the intermediate complex by interactions between the uncomplexed 2,2′-bipyridine ligands and the phosphate groups of the NADH.

Figure 7 presents a summary of the values for the heterogeneous rate constant k_{cat}. The kinetics of the catalytic oxidation of NADH depends both on the structure of metal complex and the linker. The highest values of k_{cat} were obtained for modifications with ruthenium complexes **B** and **C** with additional bidentate phendione and 2,2′-bipyridine ligand, respectively. In comparison, the values of k_{cat} obtained for electrodes modified with complex **A** with two monodentate chloride ligands tend to be the lowest for a given linker. Modifications **13–20** with tetrahedral zinc complex **D** show

intermediate values of k_{cat}, with the exception of modification **17**, which among all modifications was found to give the second highest k_{cat} of ~12 s^{-1}. These observations suggest that the presence of the additional bidentate ligands with conjugated aromatic systems increases the rate of catalytic reaction of the phendione ligand with NADH. Simply based on the redox potential values (Table 2) we should expect the values for k_{cat} for the Zn complex to be smaller than those for the Ru complexes because the thermodynamic driving force is lower. If we use the linear free energy relationship from Gorton[51] ($\log_{10}[k_2/dm^3\ mol^{-1}\ s^{-1}] = 2.97 + 0.0059[E^{0\prime}$ vs SCE/mV]) we expect k_{cat} for the Zn complexes to be around 1.5 times smaller than the values for the Ru complexes due to the ~30 mV cathodic shift in the redox potential. In practice any effect of the thermodynamic driving force appears to be obscured by other factors such as the differences in the geometry of the complexes and the effects of the other ligands. It is also notable that there does not appear to be any strong effect from the charge on the metal complexes (compare modifications **1**−**4** with neutral ruthenium complex with the other complexes which are dications).

The choice of linker was found to have a significant effect on the values of k_{cat}. For the electrodes modified with BA linker we obtain the smallest k_{cat} values irrespective of the phendione complex attached. For a given metal complex the highest values of k_{cat} are found for the EDDA linker followed by EDA; HDA shows intermediate values between these two aliphatic linkers and BA. The effects here appear to be subtle and may relate to the precise geometry of the transition state for H^- transfer in the intermediate complex.

Finally, it is worth commenting on the results for electrodes **9**−**12** with two phendione ligands as compared to electrodes **5**−**8** with only one. In our analysis we have taken Γ in eq 8 to be the surface coverage of phendione rather than the surface coverage of the complex. One could argue that the close proximity of the two phendione ligands on a single complex precludes both being involved in catalysis at the same time for a large substrate such as NADH. However, for the high surface coverages used in these experiments similar steric blocking will occur for adjacent complexes, and it therefore makes no difference whether the two adjacent phendiones are on the same molecule or on adjacent molecules. To see a significant effect one needs to go to smaller coverages, below ~10 pmol cm^{-2}, where the complexes are further apart on average than the size of the substrate.

■ CONCLUSIONS

In this work we have described the synthesis of several new complexes containing the redox active phendione ligand and their attachment at glassy carbon electrodes using a generic approach that uses a variety of different linkers and both 2,2′-bipyridine and 2-(imidazolyl)pyridine ligands. We have used this to construct a library of three replicates of each of 20 different modified electrodes using combinatorial solid-phase synthesis. This library has been screened using a multichannel potentiostat to investigate the electrochemical properties of the immobilized complexes and their propensity to catalyze the electrochemical oxidation of NADH.

We find that the coverages of the phendione complexes are related to the size of the immobilized metal complex; the smaller tetrahedral Zn(II) complexes show significantly higher coverages than the Ru(II) complexes, and among the Ru(II) complexes modifications with the less bulky bis-chloride complex **A** give the higher coverages. For a given complex we find that the choice of linker affects the coverage, with the short ethylene diamine (EDA) linker giving the highest values of surface coverage.

High-throughput methods were used to evaluate the different modified electrodes for oxidation of NADH by simultaneously recording the cyclic voltammetry for all the electrodes at several scan rates and for several concentrations of NADH. By analysis of this data using an established model for the kinetics of the mediated reaction we were able to extract the kinetic parameters k_{cat} and K_M that describe the reaction and to assess the influence of the particular complex and choice of attachment and linker on the kinetics of NADH oxidation. We find that, for the modifications studied here, the best performance is obtained for electrodes modified with the EDA linker, 2,2′-bipyridine ligand and complex **C** or the EDA linker, 2-(imidazolyl)pyridine ligand and zinc(II) complex **D**. However if we look in greater detail at the kinetics we find that the most effective complex, once the effect of coverage is taken into account, is the Ru(II) complex with one phendione and two 2,2′-bipyridine ligands attached through the EDDA linker. This suggests that the modified electrode performance might be improved by finding ways to increase the coverage of this molecule on the glassy carbon surface.

Finally, we have shown that this approach of using solid-phase synthesis methodology and high-throughput screening offers great promise as a way to investigate the relationship between structure and reactivity for chemically modified electrodes.

■ ASSOCIATED CONTENT

Supporting Information

Experimental procedures for preparation of **Impy** ligand and metal complexes **A**−**D**; solid-phase and combinatorial preparation of the 60-member library of modified electrodes **1**−**20**; cyclic voltammograms for electrodes **1**−**20** recorded in the presence and absence of NADH, plots of NADH catalytic currents i_{cat} and fitting curves at different scan rates; fitting and kinetic parameters k_{cat} and K_M for all library members. This material is available free of charge via the Internet at http://pubs.acs.org.

■ AUTHOR INFORMATION

Corresponding Author

P.N.Bartlett@soton.ac.uk (P.N.B.); j.kilburn@qmul.ac.uk (J.D.K.)

Notes

The authors declare no competing financial interest.

■ ACKNOWLEDGMENTS

The project was supported by EPSRC Grant No EP/D038588/1.

■ REFERENCES

(1) Lane, R. F.; Hubbard, A. T. *J. Phys. Chem.* **1973**, *77*, 1401.
(2) Elliott, C. M.; Murray, R. W. *Anal. Chem.* **1976**, *48*, 1247.
(3) Moses, P. R.; Wier, L.; Murray, R. W. *Anal. Chem.* **1975**, *47*, 1882.
(4) Murray, R. W. *Acc. Chem. Res.* **1980**, *13*, 135.
(5) Bard, A. J.; Stratmann, M.; Fujihira, M.; Rubinstein, I.; Rusling, J. F. *Encyclopedia of Electrochemistry: Modified Electrodes*; Wiley-VCH: Weinheim, 2007.
(6) Murray, R. W. *Molecular Design of Electrode Surfaces*; Wiley: New York, 1992.

(7) Pan, Q. M.; Wang, M.; Chen, W. T. *Chem. Lett.* **2007**, *36*, 1312.
(8) Guo, M. L.; Chen, J. H.; Zhang, Y. J.; Chen, K.; Pan, C. F.; Yao, S. Z. *Biosens. Bioelectron.* **2008**, *23*, 865.
(9) Sun, K.; Jiang, B.; Jiang, X. Y. *J. Electroanal. Chem.* **2011**, *656*, 223.
(10) Downard, A. J.; Jackson, S. L.; Tan, E. S. Q. *Aust. J. Chem.* **2005**, *58*, 275.
(11) Shedge, H. Y.; Creager, S. E. *Anal. Chim. Acta* **2010**, *657*, 154.
(12) Betelu, S.; Vautrin-Ul, C.; Chausse, A. *Electrochem. Commun.* **2009**, *11*, 383.
(13) Fan, L. S.; Chen, J.; Zhu, S. Y.; Wang, M.; Xu, G. B. *Electrochem. Commun.* **2009**, *11*, 1823.
(14) Sivanesan, A.; John, S. A. *Electroanalysis* **2010**, *22*, 639.
(15) Tanaka, H.; Aramata, A. *J. Electroanal. Chem.* **1997**, *437*, 29.
(16) Pirrung, M. C. *Chem. Rev.* **1997**, *97*, 473.
(17) Thompson, L. A.; Ellman, J. A. *Chem. Rev.* **1996**, *96*, 555.
(18) Maier, W. F.; Stowe, K.; Sieg, S. *Angew. Chem., Int. Ed.* **2007**, *46*, 6016.
(19) Potyrailo, R.; Rajan, K.; Stoewe, K.; Takeuchi, I.; Chisholm, B.; Lam, H. *ACS Comb. Sci.* **2011**, *13*, 579.
(20) Kulikov, V.; Mirsky, V. M. *Meas. Sci. Technol.* **2004**, *15*, 49.
(21) Guschin, D. A.; Shkil, H.; Schuhmann, W. *Anal. Bioanal. Chem.* **2009**, *395*, 1693.
(22) Guschin, D. A.; Castillo, J.; Dimcheva, N.; Schuhmann, W. *Anal. Bioanal. Chem.* **2010**, *398*, 1661.
(23) Chrétien, J.-M.; Ghanem, M. A.; Bartlett, P. N.; Kilburn, J. D. *Chem.—Eur. J.* **2008**, *14*, 2548.
(24) Chrétien, J.-M.; Ghanem, M. A.; Bartlett, P. N.; Kilburn, J. D. *Chem.—Eur. J.* **2009**, *15*, 11928.
(25) Sosna, M.; Chrétien, J.-M.; Kilburn, J. D.; Bartlett, P. N. *Phys. Chem. Chem. Phys.* **2010**, *12*, 10018.
(26) Downard, A. J. *Electroanalysis* **2000**, *12*, 1085.
(27) Adenier, A.; Chehimi, M. M.; Gallardo, I.; Pinson, J.; Vilà, N. *Langmuir* **2004**, *20*, 8243.
(28) Barbier, B.; Pinson, J.; Desarmot, G.; Sanchez, M. *J. Electrochem. Soc.* **1990**, *137*, 1757.
(29) Deinhammer, R. S.; Ho, M.; Anderegg, J. W.; Porter, M. D. *Langmuir* **1994**, *10*, 1306.
(30) Hoekstra, K. J.; Bein, T. *Chem. Mater.* **1996**, *8*, 1865.
(31) Bélanger, D.; Pinson, J. *Chem. Soc. Rev.* **2011**, *40*, 3995.
(32) Ghanem, M. A.; Chrétien, J.-M.; Pinczewska, A.; Kilburn, J. D.; Bartlett, P. N. *J. Mater. Chem.* **2008**, *18*, 4917.
(33) Delamar, M.; Hitmi, R.; Pinson, J.; Saveant, J. M. *J. Am. Chem. Soc.* **1992**, *114*, 5883.
(34) Pinson, J.; Podvorica, F. *Chem. Soc. Rev.* **2005**, *34*, 429.
(35) Marwan, J.; Addou, T.; Bélanger, D. *Chem. Mater.* **2005**, *17*, 2395.
(36) Coulon, E.; Pinson, J.; Bourzat, J. D.; Commerçon, A.; Pulicani, J. P. *J. Org. Chem.* **2002**, *67*, 8513.
(37) Holm, A. H.; Møller, R.; Vase, K. H.; Dong, M.; Norrman, K.; Besenbacher, F.; Pedersen, S. U.; Daasbjerg, K. *New J. Chem.* **2005**, *29*, 659.
(38) Bourdillon, C.; Delamar, M.; Demaille, C.; Hitmi, R.; Moiroux, J.; Pinson, J. *J. Electroanal. Chem.* **1992**, *336*, 113.
(39) Kariuki, J. K.; McDermott, M. T. *Langmuir* **2001**, *17*, 5947.
(40) Adenier, A.; Combellas, C.; Kanoufi, F.; Pinson, J.; Podvorica, F. I. *Chem. Mater.* **2006**, *18*, 2021.
(41) Yu, S. S. C.; Tan, E. S. Q.; T., J. R.; Downard, A. J. *Langmuir* **2007**, *23*, 11074.
(42) Westheimer, F. H.; Fisher, H. F.; Conn, E. E.; Vennesland, B. *J. Am. Chem. Soc.* **1951**, *73*, 2403.
(43) Fukuzumi, S.; Koumitsu, S.; Hironaka, K.; Tanaka, T. *J. Am. Chem. Soc.* **1987**, *109*, 305.
(44) Liang, Z.-X.; Klinman, J. P. *Curr. Opin. Struct. Biol.* **2004**, *14*, 648.
(45) Rodkey, F. L. *J. Biol. Chem.* **1955**, *213*, 777.
(46) Rodkey, F. L.; Donovan, J. A. *J. Biol. Chem.* **1959**, *234*, 677.
(47) Chenault, H. K.; Whitesides, G. M. *Appl. Biochem. Biotechnol.* **1987**, *14*, 147.
(48) Gorton, L.; Dominguez, E. In *Encyclopedia of Electrochemistry*; Wilson, G. S., Ed.; Wiley-VCH: Weinheim, 2002; p 67.
(49) Gorton, L.; Bartlett, P. N. In *Bioelectrochemistry: Fundamentals, Experimental Techniques and Applications*; Bartlett, P. N., Ed.; John Wiley & Sons: Chichester, 2008; p 157.
(50) Bartlett, P. N.; Tebbutt, P.; Whitaker, R. G. *Prog. React. Kinet.* **1991**, *16*, 55.
(51) Gorton, L. *J. Chem. Soc., Faraday Trans. 1* **1986**, *82*, 1245.
(52) Gorton, L.; Domínguez, E. *Rev. Mol. Biotechnol.* **2002**, *82*, 371.
(53) Simon, E.; Bartlett, P. N. In *Biomolecular Films: Design, Function, and Applications*; Rusling, J. F., Ed.; Marcel Dekker: New York, 2003, p 499.
(54) Carlson, B. W.; Miller, L. L. *J. Am. Chem. Soc.* **1985**, *107*, 479.
(55) Gillard, R. D.; Hill, R. E. E. *J. Chem. Soc., Dalton Trans.* **1974**, 1217.
(56) (a) Wu, Q.; Maskus, M.; Pariente, F.; Tobalina, F.; Fernandez, V. M.; Lorenzo, E.; Abruna, H. D. *Anal. Chem.* **1996**, *68*, 3688. (b) Tobalina, F.; Pariente, F.; Hernandez, L.; Abruna, H. D.; Lorenzo, E. *Anal. Chim. Acta* **1999**, *395*, 17. (c) Lei, Y.; Shi, C.; Anson, F. C. *Inorg. Chem.* **1996**, *35*, 3044. (d) Goss, C. A.; Abruňa, H. D. *Inorg. Chem.* **1985**, *24*, 4263. (e) Kou, Y. Y.; Xu, G. J.; Gu, W.; Tian, J. L.; Yan, S. P. *J. Coord. Chem.* **2008**, *61*, 3147. (f) Wang, Q. X.; Gao, F.; Jiao, K. *Electroanalysis* **2008**, *20*, 2096. (g) Darder, M.; Takada, K.; Pariente, F.; Lorenzo, E.; Abruna, H. D. *Anal. Chem.* **1999**, *71*, 5530. (h) Yokoyama, K.; Ueda, Y.; Nakamura, N.; Ohno, H. *Chem. Lett.* **2005**, *34*, 1282. (i) Popescu, I. C.; Dominguez, E.; Narvaez, A.; Pavlov, V.; Katakis, I. *J. Electroanal. Chem.* **1999**, *464*, 208. (j) Shi, M. L.; Anson, F. C. *Anal. Chem.* **1998**, *70*, 1489. (k) Hedenmo, M.; Narváez, A.; Dorníguez, E.; Katakis, I. *Analyst* **1996**, *121*, 1891.
(57) Ghanem, M. A.; Chrétien, J.-M.; Kilburn, J. D.; Bartlett, P. N. *Bioelectrochemistry* **2009**, *76*, 115.
(58) Evans, I. P.; Spencer, A.; Wilkinson, G. *J. Chem. Soc., Dalton Trans.* **1973**, 204.
(59) Note: $\Gamma = Q/nFA\rho$ where Q is charge obtained by the integration of an area under the oxidation or reduction peaks, F is the Faraday constant, A the geometric area of the electrode (0.071 cm^2), $n = 2$ is the number of electrons transferred, and ρ is the roughness of the electrode; a value of 4 has been used in all calculations.
(60) Boland, S.; Barrière, F.; Leech, D. *Langmuir* **2008**, *24*, 6351.
(61) Blaedel, W. J.; Haas, R. G. *Anal. Chem.* **1970**, *42*, 918.
(62) Samec, Z.; Elving, P. J. *J. Electroanal. Chem.* **1983**, *144*, 217.
(63) Note: Although the library of electrodes was ultimately tested using a high throughput (HTP) multichannel potentiostat, we observed during preparation of the single electrode **1** that attachment of the EDA at the GC generates currents during the first cycle in the range of 200−300 μA, whereas the HTP multichannel potentiostat used in this work had a current limit of 50 μA. Therefore, attachment of the linkers for 60 GC electrodes could not be carried out simultaneously, and instead, the electrochemical attachment of linkers was carried out individually for each GC electrode using conventional three-electrode cyclic voltammetry, which controlled attachment of the linker for each individual electrode.
(64) Note: **Impy**·TFA was prepared according to a procedure modified from Yi, H.; Crayston, J. A.; Irvine, J. T. S. *Dalton Trans.* **2003**, 685 ; see Supporting Information for details.
(65) Alessio, E. *Chem. Rev.* **2004**, *104*, 4203.
(66) Boghaei, D. M.; Behzadian-Asl, F. *J. Coord. Chem.* **2007**, *60*, 347.
(67) Zakeeruddin, S. M.; Nazeeruddin, M. K.; Humphry-Baker, R.; Grätzel, M.; Shklover, V. *Inorg. Chem.* **1998**, *37*, 5251.
(68) Huan, Z.; Persson, B.; Gorton, L.; Sahni, S.; Skotheim, T.; Bartlett, P. *Electroanalysis* **1996**, *8*, 575.
(69) Lyons, M. E.; Lyons, C. H.; Michas, A.; Bartlett, P. N. *J. Electroanal. Chem.* **1993**, *351*, 245.
(70) Nicholson, R. S.; Shane, I. *Anal. Chem.* **1964**, *36*, 706.